Available online at www.sciencedirect.com
SCIENCE DIRECT®
Journal of Solid State Chemistry 174 (2003) 241–248
JOURNAL OF SOLID STATE CHEMISTRY
http://elsevier.com/locate/jssc

Thermal stability and structural deformation of rutile SnO_2 nanoparticles

J.A. Toledo-Antonio,[a,*] R. Gutiérrez-Baez,[b] P.J. Sebastian,[a,b] and A. Vázquez[a]

[a] *Instituto Mexicano del Petróleo, Prog. de Ingeniería Molecular, Eje Central Lázaro Cárdenas, # 152 AP, 07730 México, DF, Mexico*
[b] *Centro de Investigación en Energía-UNAM, Temixco, Morelos, Mexico*

Received 22 October 2002; received in revised form 14 February 2003; accepted 3 April 2003

Abstract

Nanoparticles of rutile SnO_2 were synthesized by precipitation at room temperature. Samples were characterized with X-ray diffraction, transmission electron microscopy, thermoanalysis and nitrogen physisorption by BET method. The rutile crystalline structure was refined by Rietveld method. Crystallites had spherical morphology with crystallite sizes growing with the annealing temperature. The spherical crystallites aggregate to form grains composed of a number of crystallites defining the specific surface area and porosity. The crystallites contained hydroxyls in their structure and on their surface generating considerable amount of tin vacancy sites in the structure. These hydroxyls modify the Sn–O bonds, increase the lattice parameters and produce asymmetry in the representative rutile tin–oxygen octahedron. As the dehydroxylation was done with the annealing temperature, the atomic bond length between the oxygen atoms shared by adjacent octahedra decreased, contracting the lattice and increasing the symmetry.

Keywords: Tin oxide; Rutile crystalline structure; Bond lengths

1. Introduction

Tin oxide, SnO_2, has been used in a wide range of application in sciences, technologies and industries, such as catalysis, conductivity, gas sensing, ceramics, plastics, and biomedicine [1,2]. Recently, it has been reported that the tin oxide has good possibilities to serve as anode in Li-ion batteries [3]. These kinds of batteries are the most promising devices to accomplish the actual and nearly future requirements of portable energy and as support for the alternative energy sources, like electric engines for transportation purposes in automobiles for example. Tin oxide has shown a better performance than the carbonaceous materials, actually used as anode in those devices. However, the tin oxide (IV) has problems of cyclical Li-ion insertion for a commercial application [4]. Nevertheless, if this problem is overcome, this material would offer a real possibility to improve the Li-ion batteries performance; therefore, strong efforts must be directed to the synthesis and structural and textural properties of SnO_2 to a better understanding of its behavior.

The synthesis of SnO_2 has been done, traditionally, in two ways: (a) hydrolysis of tin (IV) salts in aqueous solutions and (b) Sn^0 oxidation with hot concentrated nitric acid. Both methods yield hydrated forms of SnO_2 [1]. Then it must be dehydrated and dehydroxylated with the annealing treatment. Recently we have shown that rutile TiO_2, with the same crystallographic structure than SnO_2, has large amount of vacancy sites generated by the hydroxyl groups incorporated into the lattice during the synthesis; these vacancy sites decreased during dehydroxylation process with the annealing temperature [5,6]. Therefore, it is interesting to elucidate the presence of these defects in SnO_2 and its influence on the ion host properties.

In this work, the structural deformation of the SnO_2 rutile was studied as a function of the annealing temperature. The vacancy sites generated by the hydroxyl groups remained in the structure and the bond length variations were determined by Rietveld method. Morphology and texture of SnO_2 were analyzed by transmission electron microscopy and nitrogen physisorption.

*Corresponding author.
E-mail address: jtoledo@imp.mx (J.A. Toledo-Antonio).

0022-4596/03/$ - see front matter © 2003 Elsevier Inc. All rights reserved.
doi:10.1016/S0022-4596(03)00181-6

2. Experimental

2.1. Sample preparation

SnO_2 was prepared by the precipitation method starting from tin tetrachloride ($SnCl_4 \cdot 5H_2O$, Aldrich), which was dissolved in deionized water. Precipitation was done at room temperature by mixing, dropwise on 100 mL of deionized water at pH 9.5, the aqueous solution containing tin complex ions and an aqueous solution of NH_4OH (J.T. Baker, 50 vol%). The white precipitate was filtered, and washed thoroughly with deionized water until it was chlorine free (silver nitrate test); then, it was dried overnight at 110°C in air (fresh sample). Thereafter, a portion of this sample was annealed in the presence of air for 2 h at 200°C, 300°C, 400°C, 500°C, 700°C, and 1000°C.

2.2. Sample characterization

2.2.1. X-ray diffraction

The X-ray diffraction pattern of the sample packed in a glass holder was recorded at room temperature with Cu$K\alpha$ radiation in a Rigaku diffractometer that had $\theta - \theta$ configuration and a graphite monochromator in the secondary beam. Diffraction intensity was measured between 10° and 70°, with a 2θ step of 0.02° for 4.0 s per point. Crystalline structures were refined with the Rietveld technique by using FULLPROF98 code [7]; peak profiles modeled with pseudo-Voigt functions [8] contained average crystallite size as one of its characteristic parameters [9]. Standard deviations, which show the last figure variation of a number, are given in parentheses. When they correspond to refined parameters, their values are not estimates of the probable error in the analysis as a whole, but only of the minimum possible probable errors based on their normal distribution [10].

2.2.2. Textural measurements

Specific surface areas were determined by nitrogen physisorption applying the BET method on an ASAP-2000 apparatus.

2.2.3. Thermoanalysis

Weight losses and the temperatures associated to phase transformations were determined by thermogravimetry with a Perkin-Elmer TG-7 apparatus; samples were heated in air flow from room temperature up to 1000°C at 10°C/min.

2.2.4. Transmission electron microscopy (TEM)

The samples milled and dispersed in ethanol before supporting them in the copper grid covered with formvar were observed at 400,000× with a JEOL 100CX transmission electron microscope that had high-resolution polar pieces.

3. Results and discussion

Poorly crystallized rutile SnO_2 was obtained by precipitation of $SnCl_4$ at low temperature, from 110°C to 300°C (Fig. 1). Crystallization of the rutile structure evolved with the annealing temperature and well-crystallized structure was obtained after annealing at 700°C (Fig. 2). Rutile unit cell with tetragonal symmetry was described with the space group $P4_2/mnm$ and the atomic position is given in Table 1. This unit cell was used in the model of the X-ray diffraction pattern for refining the crystalline structure with the Rietveld method (Fig. 3).

The peak widths of the diffraction patterns were well resolved by assuming only strain and crystallite size effect; then, crystallites grew uniformly along all directions suggesting spherical morphology, which was confirmed by transmission electron microscopy (TEM) images (Fig. 4). In fact, crystallite sizes obtained by refinement of the experimental diffraction patterns correspond very well to those measured by TEM micrographs (Table 2 and Fig. 4).

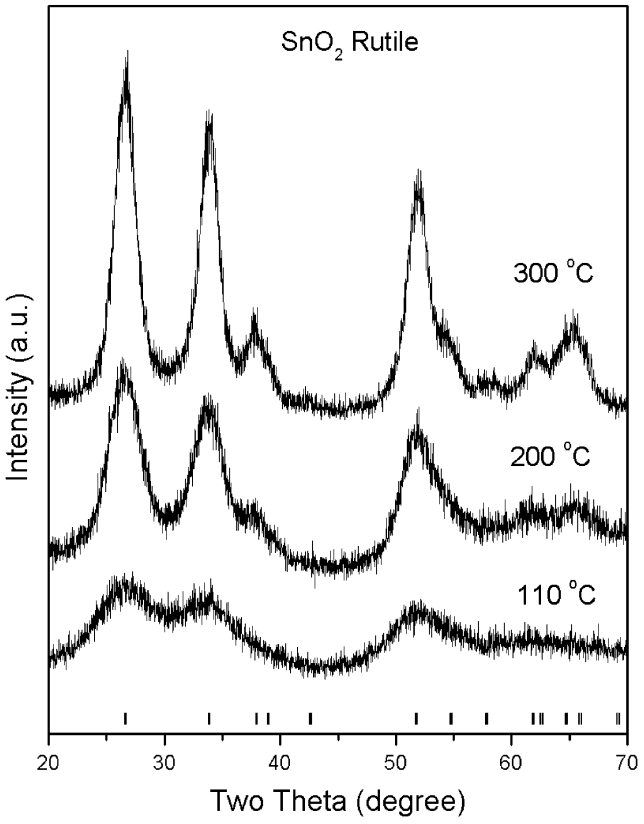

Fig. 1. X-ray diffraction patterns of the SnO_2 nanoparticles annealed at 110°C, 200°C and 300°C. The tick marks correspond to rutile SnO_2.

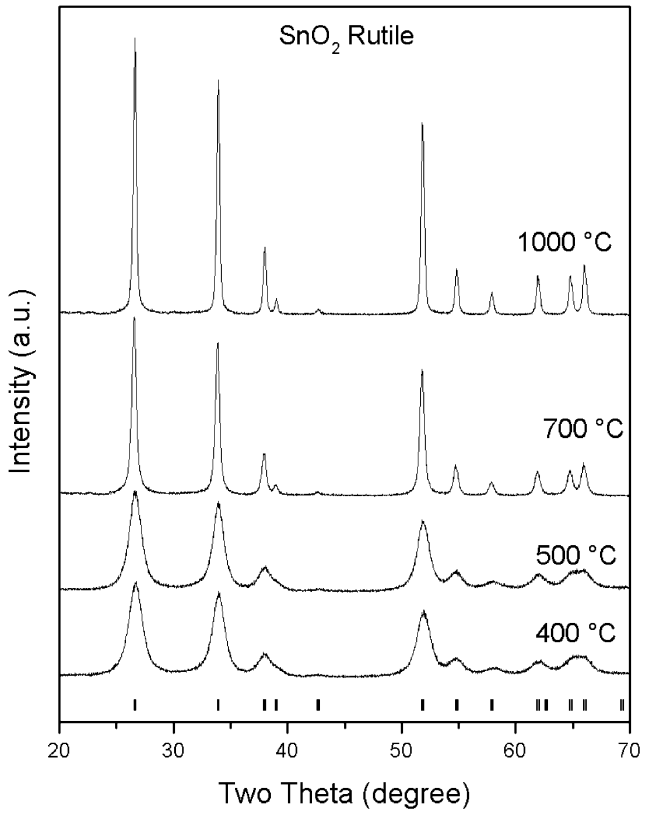

Fig. 2. X-ray diffraction patterns of the SnO_2 nanoparticles annealed from 400°C to 1000°C. The tick marks correspond to rutile SnO_2.

Table 1
Rutile, space group $P4_2/mnm$ (136): atom positions

Atom	Site	x	y	z
Sn	2*a*	0.0	0.0	0.0
O	4*f*	*u*	*u*	0.0

Fresh SnO_2 sample dried at 110°C had a very small crystallite size of 2.58(3) nm; this sample, however, had large amount of water molecules adsorbed on its surface and also considerable amount of hydroxyl groups on its structure, as was observed by thermal analysis (TGA) (Fig. 5). The first minimum peak centered at 100°C with a weight loss of 9 wt% corresponds to desorption of water molecules physisorbed on the particle surface. The second minimum peak centered at 300°C with a weight loss of 6.27 wt% corresponds to the dehydroxylation process.

SnO_2 crystallites grew smoothly as the dehydroxylation proceeded, annealing the sample from 110°C to 500°C. Up to 500°C, where practically all dehydroxylation process was done and only a residual amount of hydroxyls remained in the sample (Fig. 5), SnO_2 crystallite showed a fast growth from 8.11(7) to 23.1(3) nm for the samples annealed at 500°C and 700°C, respectively. Therefore, hydroxyls that remained in the samples inhibit the growing of the SnO_2 crystallites at temperatures below 500°C.

In the fresh sample, annealed at 110°C, a large amount of water was found to be adsorbed on the crystallite surface (Fig. 5), and it seems that it modifies its lattice parameters (Table 2); when these adsorbed water molecules were eliminated from the SnO_2 surface at 200°C, the sample showed larger a and c parameters. Thereafter, lattice parameters, a and c, decreased from 0.4768(6) to 0.47330(3) nm and from 0.3208(3) to 0.31834(2) nm for the samples annealed at 200°C and 1000°C, respectively. This decrease in lattice parameters with the annealing temperature must be attributed to the dehydroxylation of the material, suggesting the presence of large amount of the hydroxyl groups in the bulk of

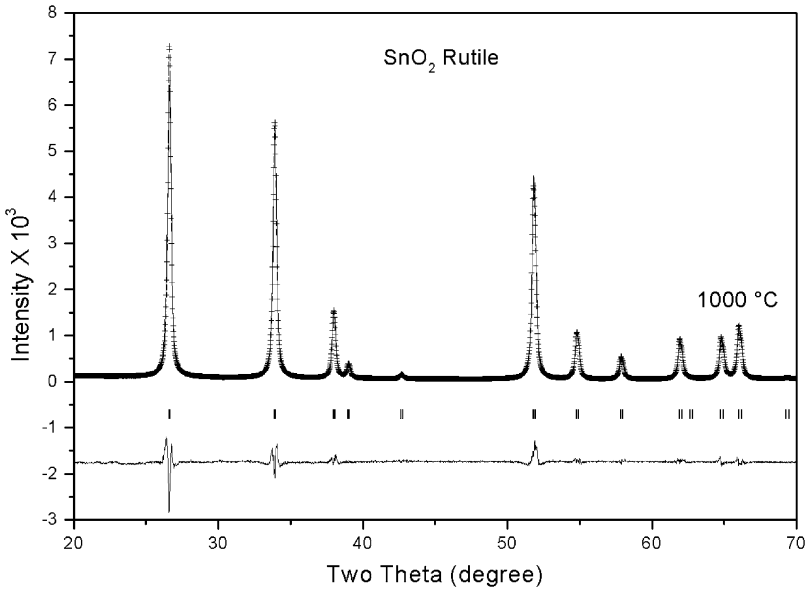

Fig. 3. Rietveld refinement plot of the samples annealed at 1000°C (Rwp = 0.155, RF = 0.00355). Crosses correspond to experimental data, continuous line, to the calculated data, and the difference between experimental and calculated data. Tick marks correspond to rutile SnO_2.

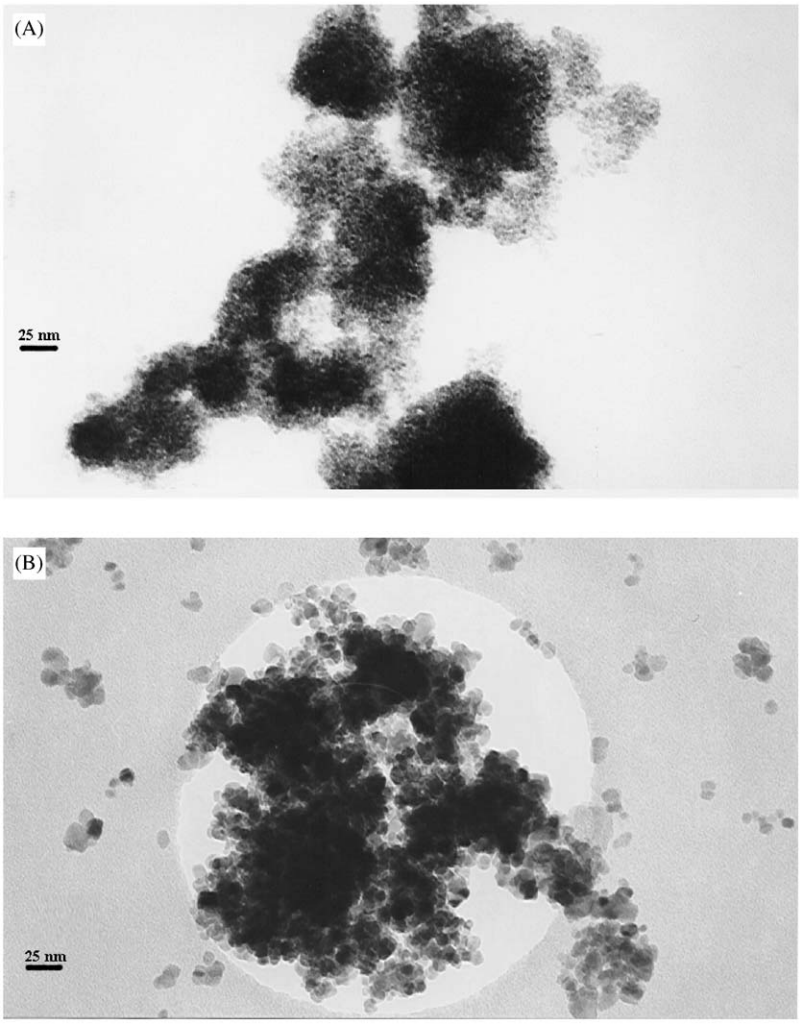

Fig. 4. Transmission electron micrographs taken at 400,000× of the samples annealed at (A) 200°C and (B) 500°C.

Table 2
Crystallite size, lattice parameters, oxygen positions and tin vacancy in SnO_2 nanoparticles

Temperature (°C)	Crystallite size (nm)	*a* (nm)	*c* (nm)	*u*	Tin vacancy (%)
Fresh	2.58(3)	0.4726(1)	0.3180(1)	0.290(2)	43(4)
200	2.73(5)	0.4769(6)	0.3208(3)	0.278(1)	44(5)
300	4.81(7)	0.4746(2)	0.3191(1)	0.291(1)	30(4)
400	7.25(7)	0.47337(9)	0.31847(7)	0.2939(9)	26(3)
500	8.11(7)	0.47326(8)	0.31839(6)	0.2943(9)	23(3)
700	23.1(3)	0.47318(4)	0.31821(3)	0.304(1)	16(3)
1000	38.3(6)	0.47330(3)	0.31834(2)	0.305(1)	10(4)

the SnO_2 crystallites, generating a bad crystallized rutile structure. In fact, this large amount of hydroxyls in the bulk of the crystallites gives rise to a large amount of Sn vacancy sites (Table 2), which decreased from 44(5)% to 10(3)% on annealing the sample from 200°C to 1000°C, respectively. TiO_2 rutile synthesized at low temperature also had a concentration of 16% of vacancy sites in its structure, which decreased to 8% annealing at 1000°C [5]; however, when TiO_2 rutile was doped with SnO_2, the amount of vacancy sites practically disappeared [6]. Though SnO_2 rutile crystallite size was very low, it had large amount of Sn vacancy sites if compared with that for TiO_2 rutile structure, Table 2 and Refs. [5,6]. The latter suggest that SnO_2 retains a larger amount of

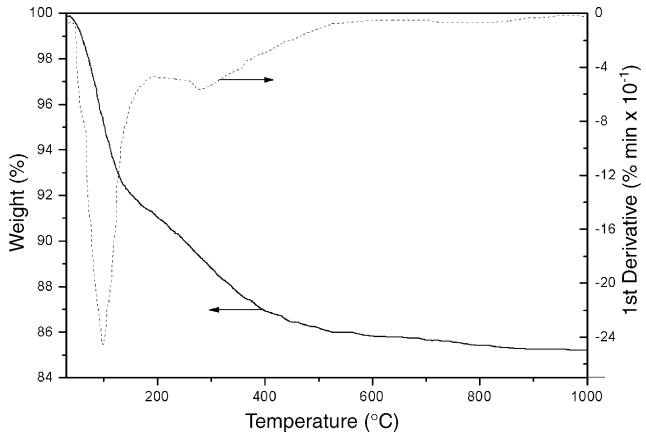

Fig. 5. Thermogravimetric and first derivative curves of the fresh SnO_2 sample annealed in air at 10°C/min.

hydroxyls on its structure than TiO_2; in fact, it has been demonstrated that SnO_2 retains hydroxyl groups, still annealing at 1500°C [1].

Oxygen positions u of the rutile SnO_2 structure also change with the annealing temperature; it changed from 0.278(1) to 0.305(1) on annealing from 200°C to 1000°C, respectively, Table 2. This suggests that strong crystal deformation must be occurring in the SnO_2 rutile structure. Therefore, a careful analysis of the local order structure must be necessary.

The representative polyhedron of the rutile SnO_2 structure (Fig. 6) is formed by a tin atom in the center, surrounded by six oxygen atoms in the vertex. The tin atom is bonded to four oxygen atoms with the same bond length (R4) in the basal plane and with another two apical oxygen atoms with a bond length (R5). R1 and R2 were labeled as the distance between two oxygen atoms sharing the vertex of the basal plane of the polyhedron (Fig. 6), while R3 is the distance between the apical oxygen atoms and the oxygen atoms of the basal plane of the polyhedron. All latter distances are reported in Table 3. Both Sn–O bond lengths (R4 and R5) showed an asymmetrical deformation of the polyhedra in fresh and low-temperature-annealed samples; this structural deformation of the octahedron tends to a higher symmetry as dehydroxylation proceeded; the higher symmetry was reached on annealing the sample at 700°C; thereafter, both Sn–O bond lengths remained constant. In other words, the four Sn–O bonds of the basal plane decreased while the two apical Sn–O bonds increased, giving rise to an R4/R5 ratio close to 1.0 for the samples annealed up to 700°C (Table 3; Fig. 8). Contrary to that previously reported for rutile TiO_2 [5,6], higher symmetry of the characteristic octahedron was attained for the fresh and low-temperature-annealed samples, which had large amount of hydroxyls in the structure. In this case, however, the four Ti–O bonds of the basal plane are lower than the two apical Ti–O

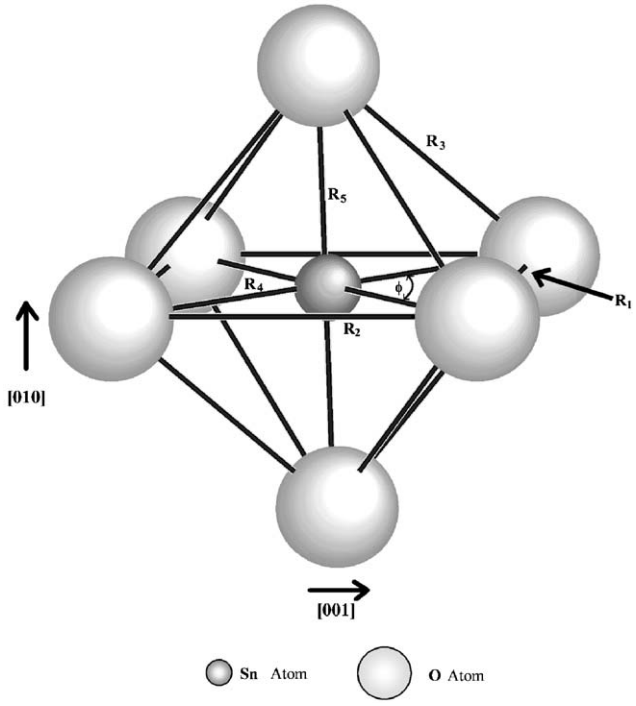

Fig. 6. Representative polyhedron of the rutile crystalline structure of tin (IV) oxide. The atomic bond lengths are presented in Table 3.

bonds, whereas, in SnO_2 rutile the two apical Sn–O bonds are lower than the four Sn–O bonds of the basal plane. These characteristic differences between both SnO_2 and TiO_2 structures suggest that hydroxyl groups interact with the oxygen atoms bonded with tin or titanium atoms relaxing the Sn–O or Ti–O bonds at the basal plane (R4) of the octahedral with the consequent contraction of the two apical Sn–O or Ti–O bonds (R5); as the annealing temperature rose, the hydroxyl groups came to be eliminated with the consequent sintering of the crystallites; the four Sn–O bonds decreased while the two apical Sn–O bonds rose, increasing the symmetry of the characteristic octahedron because R4 tends to equal R5 dimensions. In the case of TiO_2 structure, the hydroxyl groups also relax the four Ti–O bonds at the basal plane of the polyhedron, resulting similar to the two apical Ti–O bonds and higher symmetry is obtained at low temperature when hydroxyls remain in the structure. These results suggest that hydroxyl groups that remained in rutile induce structural deformation and bond length variations.

The structural deformation of the SnO_2 was also reflected in the O–Sn–O angle (ϕ) formed by two Sn–O bonds in the basal plane (Fig. 6). This angle decreased from 85.98(2) to 78.88(2) when the samples were annealed from 200°C to 1000°C respectively (Table 3). The decrease in this (ϕ) angle suggests that the corresponding O–O distance (R1) must decrease; in fact, larger variation in the polyhedron was observed

Table 3
Atomic bond lengths and the atomic bond angle ϕ in rutile SnO_2 (Fig. 6)

T (°C)	R1	R2	R3	R4	R5	R6	R4/R5	ϕ (deg)
Fresh	0.28062(7)	0.31814(5)	0.28740(6)	0.21211(6)	0.19392(7)	0.33851(7)	1.0938(6)	82.83(2)
200	0.29903(7)	0.32079(5)	0.28863(6)	0.21928(6)	0.18769(7)	0.33936(7)	1.1683(6)	85.98(2)
300	0.28107(7)	0.31914(5)	0.28853(6)	0.21263(6)	0.19503(7)	0.33996(7)	1.0902(6)	82.74(2)
400	0.27597(7)	0.31848(5)	0.28830(6)	0.21071(6)	0.19677(7)	0.33987(7)	1.0708(5)	81.81(2)
500	0.27521(7)	0.31838(5)	0.28827(6)	0.21042(6)	0.19704(7)	0.33988(7)	1.0679(4)	81.68(2)
700	0.26178(7)	0.31821(5)	0.28972(6)	0.20603(6)	0.20370(7)	0.34242(7)	1.0114(4)	78.88(2)
1000	0.26185(7)	0.31834(5)	0.28981(6)	0.20610(6)	0.20375(7)	0.34251(7)	1.0115(4)	78.88(2)

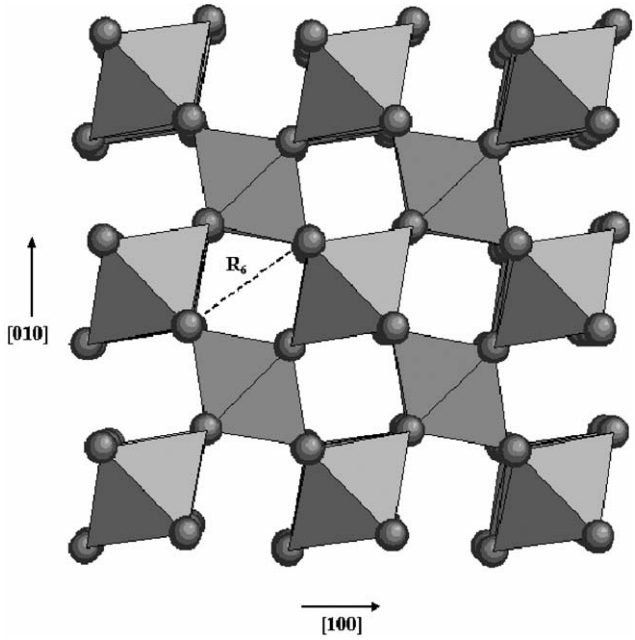

Fig. 7. Projection of rutile's crystalline structure on a plane perpendicular to [001] direction.

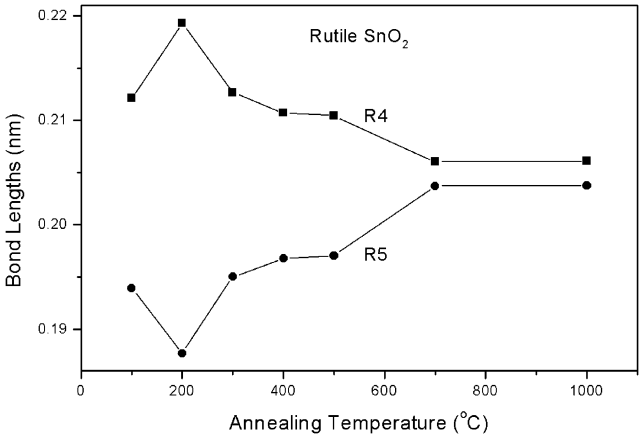

Fig. 8. Atomic bond length (Sn–O) variations as a function of annealing temperature.

in R1 dimensions, which correspond to the edges shared between continuous octahedra. It decreased from 0.29903(7) to 0.26185(7) nm for the sample annealed at 200°C and 1000°C, respectively (Table 3). The other two O–O distances of the polyhedra, R2 and R3 (Table 3), showed only slight variation in the presence of the hydroxyl groups. In fact, R2 distance is a unit cell in c plane and this varied lesser than a and b unit cells. These variations in O–O dimensions could be explained as a function of the oxygen position (u) variation only along x and y directions.

The decrease in O–O (R1) distance and O–Sn–O (ϕ) angle means that the polyhedron became thinner in the plane perpendicular to c-axis. These octahedra share only two edges, forming octahedra filaments parallel to [001] direction [11] and these filaments are connected between each other along [110] directions via the octahedra vertices (R1 distance) (Figs. 7 and 8), generating atom-free tunnels along [001] direction. If the polyhedra became thinner by an increase in R1 O–O distance, the square cross section of the tunnels also must change; this was measured as the distance between two oxygen atoms in the diagonal of the tunnels and it was named R6, also reported in Table 3. This O–O (R6) distance varied from 0.33851(7) to 0.34251(7) nm for the fresh and 1000°C annealed samples, respectively. These results suggest that the presence of hydroxyls slightly close to the atom-free tunnels allow having cations in tunnels (such as Li^+ ion) that can make a bond length with oxygen atoms (Li–O) of about 0.2 nm.

It is well known that during dehydroxylation, strong sintering occurs in the material; hence, it is interesting to know how this phenomenon affects the specific surface area and pore size distribution, which are important parameters to be taken into account when this material is used as ion host or as catalyst. Analyzing the hysteresis loop shape of the nitrogen isotherms (Fig. 9), information about pore blocking and pore structure can be obtained in SnO_2 samples. SnO_2 did not show hysteresis loop when it was annealed at 200°C; the isotherm presented in these samples corresponds to type I in the Brunauer Deming Deming and Teller (BDDT) classification [12]; it is often called a Langmuir isotherm and is observed in physisorption on a solid having fine pores; this kind of isotherms rarely occurs in

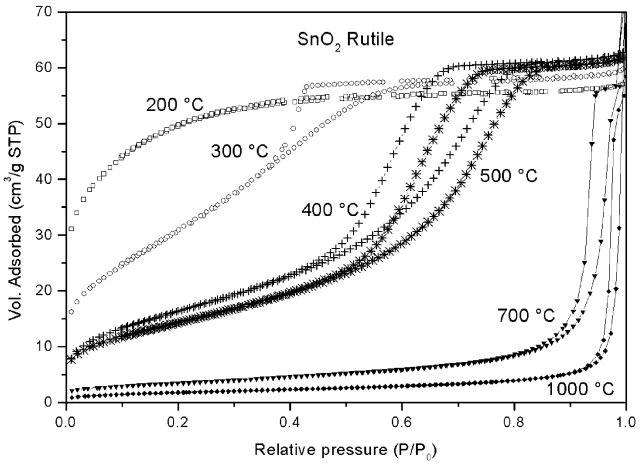

Fig. 9. Nitrogen adsorption–desorption isotherms in SnO_2 nanoparticles.

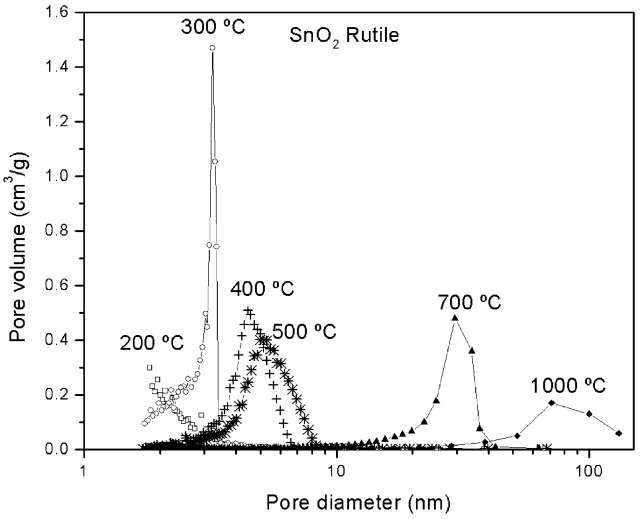

Fig. 10. Pore size distribution of SnO_2 nanoparticles.

non-porous solids [13]. The isotherms observed in the samples annealed between 300°C and 500°C corresponded to type IV in DBBT classification often observed in porous solids; the initial slopping character on the descending boundary curves reflects porous structure shrinkage cased by the stress change of the condensate during depressurization. This means that SnO_2 consisted of particles made by aggregates or agglomerates of spherical particles, such as observed by transmission electron microscopy (Fig. 4). The hysteresis loop moved to a higher relative pressure with the annealing temperature and is attributed to the non-uniform size and shape of pores (Fig. 10). The plateau of the descending boundary curves indicates an appreciable pore blockage. Moreover, the hysteresis loop would suggest that an ink-bottle pore shape was formed between aggregates with the annealing temperature. In fact, the SnO_2 annealed at 300°C had homogeneous mesopores with dimensions centered at 3 nm (Fig. 10; Table 4). Pore diameters increased with increase in the annealed temperature and the homogeneity of the pore dimension decreased.

At increasing annealing temperatures at 700°C and 1000°C, when hydroxyls have been practically eliminated from the sample and the structural symmetry was higher, the porous structure shrinkage that occurred during depressurization practically disappeared, suggesting homogeneous and cylindrical pore shapes (Fig. 10). The thinner plateau showed by the descending boundary curves indicated rigid structures without pore blockage [14]. The dimensions of the pores were 30 and 70 nm for the SnO_2 annealed at 700°C and 1000°C, respectively (Fig. 10; Table 4).

The specific surface area decreased as annealing temperature increased (Table 4), due to the strong sintering occurring in the material. However, as SnO_2 crystallites had spherical morphology (Fig. 4), and from the crystallite size determined by Rietveld analysis of the XRD patterns, the theoretical surface area exposed by the crystallites was determined (Table 4). The specific surface area measured by BET method (Table 4) was lower than that determined from the crystallite size; therefore, the surface area was not determined by the SnO_2 crystallite size but by its grain size, which was composed of a number of crystallites.

Table 4
Specific surface area and porosity of the SnO_2 nanoparticles

Annealing temperature (°C)	XRD surface area (m^2/g)	BET surface area (m^2/g)	Average pore diameter (nm)	Pore volume (cm^3/g)
110	332	190.7	2.50	0.043
200	314	169.3	2.33	0.050
300	178	92.3	2.79	0.096
400	118	50.8	4.36	0.098
500	105	44.9	5.02	0.096
700	37	11.3	22.72	0.088
1000	22	5.5	43.2	0.063

4. Conclusions

Spherical nanoparticles of rutile SnO_2 were obtained by precipitating $SnCl_4$ at room temperature in aqueous solution. These crystallites contained hydroxyls in its lattice and around it, which generated tin vacancies into the structure. When samples were annealed the tin vacancy sites decreased as consequence of the dehydroxylation process. The presence of hydroxyls in the material contributed to an enhancement of the lattice parameters and also to change oxygen positions in the SnO_2 rutile structure, which changed the symmetry of

the representative tin-oxygen octahedron. The tin-oxygen bond lengths shared by adjacent octahedral decreased with the dehydroxylation and the lattice are contracted. Higher symmetry of the representative octahedron was reached at temperatures up to 700°C when the samples were free in hydroxyls. Therefore, hydroxyls interact with the oxygen atoms deforming the structure by relaxing the Sn–O bonds at the basal plane of the representative octahedral with the consequent contraction of the apical Sn–O bonds. Specific surface area, pore size and shape depended on the grain size which could be composed of a number of crystallites which at the same time depended on the annealing temperature, the dehydroxylation degree and the crystallites sintering.

Acknowledgments

The authors would like to thank Mrs. R.I. Conde Velasco for her technical assistance. The financial support for this work was given through the projects G38618-U (CONACYT, Mexico) and D.01234 (Instituto Mexicano del Petróleo).

References

[1] P.G. Harrison, Ph.D. DSchond. Chemistry of Tin. University of Notthingham, 1989 (Chapter 4, 12 and 13).
[2] A. Hattori, Y. Tokihisa, H. Tada, S. Ito, J. Electrochem. Soc. 141 (2000) 1589.
[3] C.A. Vincent, Solid State Ion. 134 (2000) 1959.
[4] M. Mohamedi, S.J. Lee, D. Takahashi, M. Nishizawa, T. Itoh, I. Uchida, Electrochim. Acta 46 (2001) 1161.
[5] X. Bokhimi, F. Pedraza, A. Morales, J. Solid State Chem. 169 (2002) 176.
[6] J.A. Toledo Antonio, F. Pedraza, X. Bokhimi, Solar Energy Mat. & Solar Cells (2003), in press.
[7] J. Rodríguez-Carbajal, Laboratoire Leon Brillouin (CEA-CNRS), France (Tel.: +33-1-6908-3343, fax: +33-1-6908-8261, E-mail: juan@llb.saclay.cea.fr).
[8] P. Thompson, D.E. Cox, J.B. Hasting, J. Appl. Crystallogr. 20 (1987) 79.
[9] R.A. Young, P. Desai, Arch. Nauk. Mater. 10 (1989) 71.
[10] E. Prince, J. Appl. Crystallogr. 14 (1981) 157.
[11] X. Bokhimi, A. Morales, M. Aguilar, J.A. Toledo Antonio, F. Pedraza, Int. J. Hydrogen Energy 26 (2001) 1279.
[12] S. Brunauer, L.S. Deming, W.E. Deming, E. Teller, J. Am. Chem. Soc. 38 (1940) 1723.
[13] A. Baiker, Int. Chem. Eng. 25 (1985) 16.
[14] M.L. Guzman-Castillo, X. Bokhimi, J.A. Toledo Antonio, J. Salmones, F. Hernández-Beltrán, J. Phys. Chem. B 105 (2001) 2099.